

Cyclostreptin binds covalently to microtubule pores and luminal taxoid binding sites

Rubén M Buey^{1,9}, Enrique Calvo^{2,9}, Isabel Barasoain¹, Oriol Pineda³, Michael C Edler⁴, Ruth Matesanz¹, Gemma Cerezo⁵, Christopher D Vanderwal⁶, Billy W Day⁷, Erik J Sorensen⁸, Juan Antonio López², José Manuel Andreu¹, Ernest Hamel⁴ & J Fernando Díaz¹

Cyclostreptin (1), a natural product from *Streptomyces* sp. 9885, irreversibly stabilizes cellular microtubules, causes cell cycle arrest, evades drug resistance mediated by P-glycoprotein in a tumor cell line and potently inhibits paclitaxel binding to microtubules, yet it only weakly induces tubulin assembly. In trying to understand this paradox, we observed irreversible binding of synthetic cyclostreptin to tubulin. This results from formation of covalent crosslinks to β -tubulin in cellular microtubules and microtubules formed from purified tubulin in a 1:1 total stoichiometry distributed between Thr220 (at the outer surface of a pore in the microtubule wall) and Asn228 (at the luminal paclitaxel site). Unpolymerized tubulin was only labeled at Thr220. Thus, the pore region of β -tubulin is an undescribed binding site that (i) elucidates the mechanism by which taxoid-site compounds reach the kinetically unfavorable luminal site and (ii) explains how taxoid-site drugs induce microtubule formation from dimeric and oligomeric tubulin.

The mitotic spindle is an important target in cancer chemotherapy¹. Spindle function is dependent on microtubule dynamics, which involves stochastic gain and loss of $\alpha\beta$ -tubulin heterodimers from microtubule ends. Growth or shortening depends on the activation state of tubulin, which is controlled by the exchangeable nucleotide bound to the β subunit. "Activated" tubulin-GTP adds to microtubule ends, whereas "deactivated" tubulin-GDP dissociates from polymer ends and does not normally polymerize into microtubules.

Compounds that bind to tubulin arrest cells in mitosis and cause apoptosis. These agents interfere with microtubule dynamics even at intracellular concentrations far below the tubulin concentration². Inhibitors of assembly (such as colchicine; **2**) inactivate tubulin, thereby preventing microtubule formation. In contrast, microtubule stabilizing agents (MSAs) such as paclitaxel bind preferentially to assembled tubulin, thereby minimizing dissociation of tubulin-GDP from microtubule ends³. MSAs also induce assembly of the otherwise inactive tubulin-GDP⁴. In recent years, many structurally diverse taxoid-site MSAs have been discovered, including epothilone B and discodermolide, which are biochemically more potent than paclitaxel⁵, and cyclostreptin (FR182877; **Fig. 1a**), which, though apparently less active than paclitaxel, has unusual biochemical properties⁶.

Paclitaxel-stabilized, zinc-induced sheets of antiparallel tubulin protofilaments have been used for construction of a model of tubulin

with bound paclitaxel⁷. After fitting this model into electron density microtubule maps, investigators concluded that paclitaxel binds to β -tubulin facing the microtubule lumen⁸. This model is supported by tubulin mutation data from cells that are resistant to paclitaxel and epothilones⁹.

Two points remain obscure about the biochemical mechanism by which taxoid-site ligands induce tubulin assembly. First, examination of the binding kinetics of paclitaxel¹⁰ yields a high kinetic association constant ($k_f = 3.6 \times 10^6 \text{ M}^{-1} \text{ s}^{-1}$), which is inconsistent with a relatively inaccessible luminal binding site. An exposed site is also supported by microtubule-associated protein (MAP)-mediated reduction in the paclitaxel binding rate¹⁰ and by the binding of antifluorescein antibody to a fluorescein-labeled taxoid bound to microtubules¹¹. These findings led us to propose an initial binding site for paclitaxel on the outer microtubule wall near pore type I, which is close to the luminal site, followed by translocation of the drug to its luminal site¹⁰. Because there is 1:1 stoichiometry for paclitaxel binding to $\alpha\beta$ -tubulin, the two sites must be mutually exclusive, perhaps with a shared element.

Second, although apparently the paclitaxel site exists only in assembled microtubules¹², taxoid-site drugs can induce microtubule assembly under conditions in which tubulin is normally unable to assemble; thus, no binding sites can be demonstrated. Therefore, given

¹Centro de Investigaciones Biológicas, Consejo Superior de Investigaciones Científicas, Ramiro de Maeztu 9, Madrid 28040, Spain. ²Unidad de Proteómica, Centro Nacional de Investigaciones Cardiovasculares, Melchor Fernández Almagro 3, Madrid 28029, Spain. ³Departament de Química Orgànica, Facultat de Química, Universitat de Barcelona, Av. Diagonal 647, Barcelona 08028, Spain. ⁴Toxicology and Pharmacology Branch, Developmental Therapeutics Program, Division of Cancer Treatment and Diagnosis, National Cancer Institute at Frederick, National Institutes of Health, Frederick, Maryland 21702, USA. ⁵PharmaMar, S.A. Avda. de los Reyes 1, Colmenar Viejo 28770, Spain. ⁶Department of Chemistry, University of California, Irvine, California 92697, USA. ⁷Departments of Pharmaceutical Sciences and Chemistry, University of Pittsburgh, Pittsburgh, Pennsylvania 15261, USA. ⁸Department of Chemistry, Princeton University, Princeton, New Jersey 08544, USA. ⁹These authors contributed equally to this work. Correspondence should be addressed to J.F.D. (fer@cib.csic.es).

Received 20 July 2006; accepted 8 December 2006; published online 7 January 2007; doi:10.1038/nchembio853

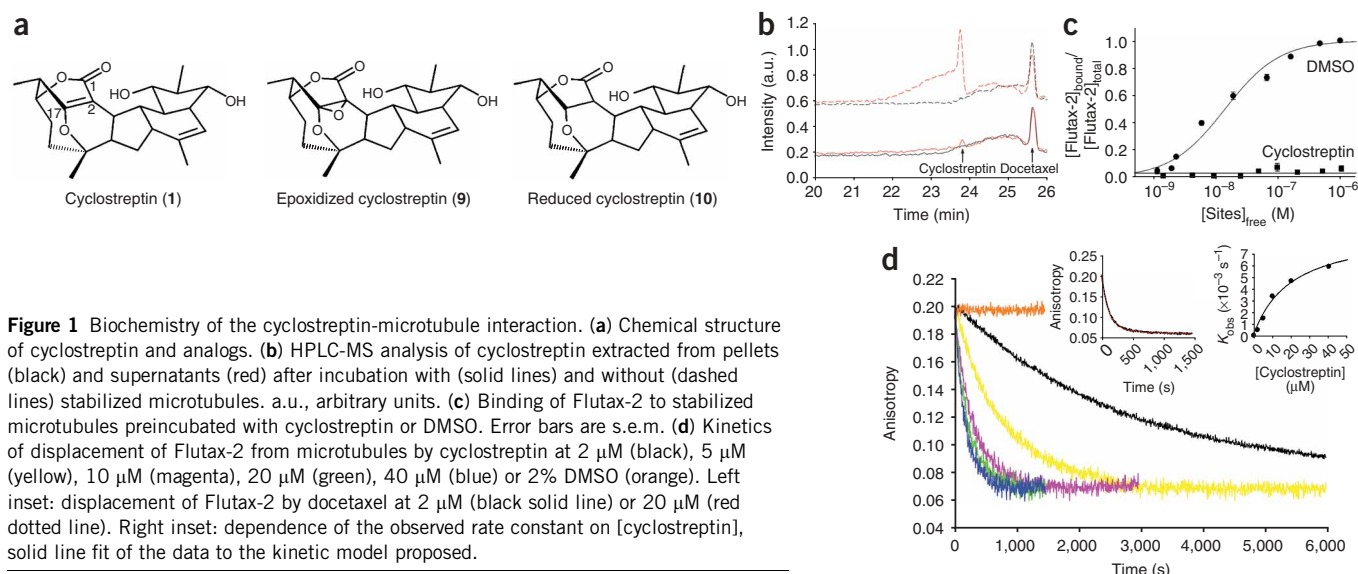


Figure 1 Biochemistry of the cyclostreptin-microtubule interaction. **(a)** Chemical structure of cyclostreptin and analogs. **(b)** HPLC-MS analysis of cyclostreptin extracted from pellets (black) and supernatants (red) after incubation with (solid lines) and without (dashed lines) stabilized microtubules. a.u., arbitrary units. **(c)** Binding of Flutax-2 to stabilized microtubules preincubated with cyclostreptin or DMSO. Error bars are s.e.m. **(d)** Kinetics of displacement of Flutax-2 from microtubules by cyclostreptin at 2 μM (black), 5 μM (yellow), 10 μM (magenta), 20 μM (green), 40 μM (blue) or 2% DMSO (orange). Left inset: displacement of Flutax-2 by docetaxel at 2 μM (black solid line) or 20 μM (red dotted line). Right inset: dependence of the observed rate constant on [cyclostreptin], solid line fit of the data to the kinetic model proposed.

that assembly occurs, we postulated that there is a low-affinity binding site in tubulin dimers or oligomers that cannot be demonstrated because of low paclitaxel solubility¹².

Although cyclostreptin¹³ weakly stimulates tubulin assembly, it avidly binds to microtubules, thereby strongly inhibiting the binding of other MSAs to polymer. In addition, cyclostreptin-stabilized microtubules disassemble at 0 °C more slowly than paclitaxel-stabilized microtubules⁶. We have now found that cyclostreptin interacts covalently both *in vitro* and in cells with polymerized tubulin, blocking the binding of even the most potent taxoid-site ligands. Moreover, cyclostreptin is fully active in multidrug-resistant (MDR) ovarian carcinoma (A2780/AD) cells overexpressing P-glycoprotein, which indicates that covalent binding might be a way to overcome MDR. Using HPLC-MS, we found that two amino acid residues, Thr220 and Asn228, are modified in polymerized β -tubulin (Asn228 is near the taxoid site facing the microtubule lumen; Thr220 abuts pore type I), but only Thr220 is modified when cyclostreptin interacts with unpolymerized tubulin.

RESULTS

Cyclostreptin binds irreversibly to microtubules

Because cyclostreptin strongly inhibits binding of taxoid-site ligands to microtubules, we tried to detect microtubule-bound cyclostreptin. We analyzed cyclostreptin-treated microtubules by HPLC-MS. Controls showed that cyclostreptin should have been detectable, but the pellet extracts were devoid of the compound (**Fig. 1b**). Ligand in the supernatant was greatly reduced following incubation of cyclostreptin with microtubules. In the absence of degradation products, cyclostreptin must have reacted irreversibly with the protein.

Cyclostreptin blocks binding of taxoid-site ligands

We examined competition among taxoid-site ligands having different affinities for microtubules (discodermolide (**3**), epothilone B (**4**), epothilone A (**5**), cyclostreptin and paclitaxel (**6**); K_d at 35 °C of 0.18, 1.3, 28, 49 and 70 nM, respectively)^{5,6,14}. The competition experiments were performed by adding labeled competitor before or after unlabeled ligand (**Table 1**). All ligands except cyclostreptin behaved as expected if binding reversibly to the same site (order of ligand addition had no effect). With cyclostreptin, the feeble inhibition

of discodermolide and epothilone B binding and the strong inhibition of paclitaxel binding without a preincubation became near total inhibition with a preincubation. We also examined the binding to microtubules of 7-O-[N-(2,7-difluoro-4-fluoresceincarbonyl)-L-alanyl]paclitaxel (Flutax-2; **7**), a fluorescent analog of paclitaxel¹⁵, which bound with an apparent K_d of 14 nM, but not to microtubules preincubated with cyclostreptin (**Fig. 1c**).

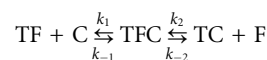
Cyclostreptin and taxanes bind by different mechanisms

Cyclostreptin can displace Flutax-2 from stabilized microtubules with an apparent K_a similar to those of paclitaxel and docetaxel (**8**)⁶. To determine whether the same mechanism is involved¹⁵, we compared the effects of docetaxel and cyclostreptin on the kinetics of Flutax-2 dissociation (**Fig. 1d**).

Docetaxel displaces Flutax-2 from microtubules because $k_f[\text{docetaxel}] \gg k_r$ (ref. 15). With any excess [docetaxel], every empty site is rapidly filled by docetaxel (**Fig. 1d**). The Flutax-2 k_r determined here was $8.9 \pm 0.3 \times 10^{-3} \text{ s}^{-1}$ at 2 μM and 20 μM docetaxel, which is in agreement with the previously determined value¹⁵ of $7.10 \pm 4 \times 10^{-3} \text{ s}^{-1}$ (error is s.e.m. for both values).

Cyclostreptin was very different. Although 2–40 μM cyclostreptin fully displaced bound Flutax-2 following monoexponential kinetic curves (**Fig. 1d**), the observed dissociation rate constant (k_{obs}) increased with cyclostreptin concentration until it equaled the k_r of Flutax-2 obtained with docetaxel (**Fig. 1d**). This indicates that the overall reaction is limited by the rate of cyclostreptin binding to microtubules. The explanation that cyclostreptin binds relatively slowly, with rebinding of free Flutax-2, is inconsistent with the monoexponential kinetic curves. These indicate a constant reaction rate, whereas increasing Flutax-2 concentration should cause the apparent k_r to decrease over time.

An alternative explanation is that cyclostreptin binds to the Flutax-2-microtubule complex and induces Flutax-2 dissociation:



where T represents the taxoid site in microtubules, C is cyclostreptin and F is Flutax-2. In this case the observed reaction step would be the second, with monophasic kinetics at steady state (concentration of

Table 1 Dependence on order of ligand addition for the binding of discodermolide, paclitaxel and epothilone B to the taxoid site

	Binding ^a of 2 μM					
	³ H]Discodermolide		¹⁴ C]Epothilone B		³ H]Paclitaxel	
	A	B	A	B	A	B
(20 μM)	Percentage of radioactive compound bound ^b \pm s.d.					
Cyclostreptin	96 \pm 4	19 \pm 6	79 \pm 10	12 \pm 1	60 \pm 2	25 \pm 2
Epothilone A	95 \pm 1	96 \pm 5	49 \pm 1	49 \pm 1	46 \pm 3	49 \pm 1
Epothilone B	76 \pm 1	79 \pm 5	9 \pm 2	9 \pm 1	31 \pm 1	33 \pm 4
Discodermolide	27 \pm 1	31 \pm 10	ND	ND	ND	ND

^aA columns: the radiolabeled ligand was added before the nonradiolabeled competitor. B columns: the nonradiolabeled competitor was added before the radiolabeled ligand. ^bThe values represent the amount of radiolabeled compound bound in the presence of the competitor relative to the amount of compound bound in its absence. ND, not determined.

TCF constant during the experiment) and the rate dependent on [cyclostreptin]. Curve fitting¹⁶ to this kinetic model yielded a k_2 value of $0.008 \pm 0.002 \text{ s}^{-1}$ (which is in agreement with the 0.006 s^{-1} value for Flutax-2 dissociation at 25 °C with docetaxel¹⁵), a negligible k_{-1} value and a k_1 value of $350 \pm 20 \text{ M}^{-1} \text{ s}^{-1}$ (errors are s.e.m.). These values indicate that an irreversible reaction has occurred.

Cellular effects of cyclostreptin

We performed competition experiments between cyclostreptin and Flutax-2 using unfixed cytoskeletons from potoroo kidney (PtK2) cells. When cyclostreptin or paclitaxel was added to cytoskeletons with bound Flutax-2, both compounds displaced Flutax-2. PtK2 cytoskeletons preincubated with paclitaxel, but not those preincubated with cyclostreptin, bound Flutax-2 (Fig. 2a–c), thereby demonstrating irreversible binding of cyclostreptin to the cytoskeletons.

Similarly, there were differences in the effects of cyclostreptin and paclitaxel on cellular microtubules. We observed partial recovery of the microtubule network in paclitaxel-treated PtK2 cells, but the effects of cyclostreptin were irreversible. Cells were incubated for 7 h with 2 or 5 μM cyclostreptin or 10 μM paclitaxel, extensively washed and incubated for 16 h or 48 h longer. Untreated cells had typical micro-

tubule networks and normal nuclei after 7 h (Fig. 2d). Cells incubated for 7 h with ligand had microtubule bundles (Fig. 2e,f), and a small percentage of them were micronucleated (4% of the cells) or arrested in mitosis with multiple asters.

After washing and another 16 h in culture, untreated cells had typical microtubule networks (Fig. 2g) and normal nuclei, whereas in the treated cells the cyclostreptin effect had progressed: the bundles were unchanged (Fig. 2h), and cells with micronucleation or multipolar spindles had increased in number to about 70%. With paclitaxel, microtubules had reverted to a normal appearance (Fig. 2i), but

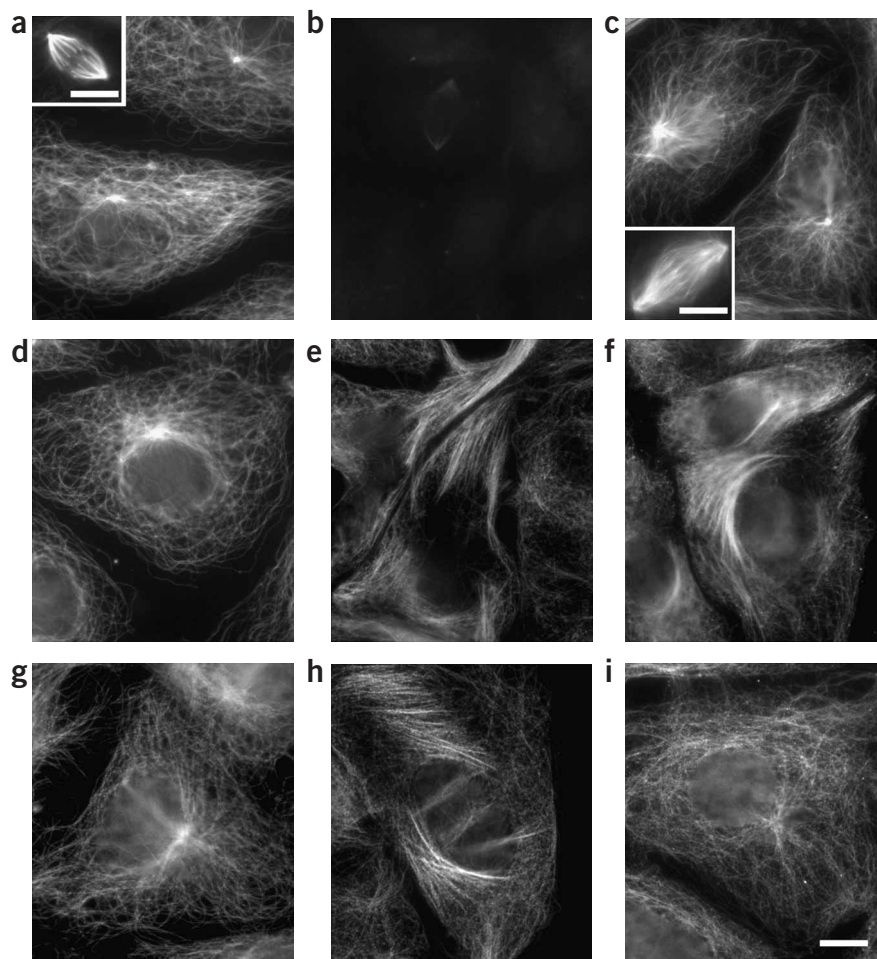


Figure 2 Inhibition of binding of Flutax-2 to PtK2 cytoskeletons by preincubation with cyclostreptin and irreversibility of microtubule effects on PtK2 cells grown in cyclostreptin. (a–c) Cytoskeletons were preincubated with DMSO (a), 10 μM cyclostreptin (b) or 10 μM paclitaxel (c) and stained with Flutax-2. Insets: Flutax-2-stained mitotic spindles from same cytoskeleton preparations. (d–f) Cells cultured for 7 h in the presence of DMSO (d), 5 μM cyclostreptin (e) or 10 μM paclitaxel (f) and immunostained. (g–i) Cells washed after 7 h, left in culture for 16 h and immunostained; shown are the DMSO treatment (g), cyclostreptin treatment (h) and paclitaxel treatment (i). Scale bar represents 10 μm , and all panels and insets have the same magnification.

Table 2 Effects of cyclostreptin compared with paclitaxel and docetaxel on the growth of human carcinoma cells

Compound	IC ₅₀ (nM) ± s.d. ^a					
	Cell line					
	A2780	A2780/AD	1A9	PTX10	PTX22	A549
Paclitaxel	1.0 ± 0.3	900 ± 200 (900) ^b	1.1 ± 0.2	30 ± 9 (27)	19 ± 5 (17)	3.6 ± 0.4
Docetaxel	0.5 ± 0.1	285 ± 60 (570)	0.6 ± 0.1	ND	ND	7.2 ± 0.3
Cyclostreptin	43.5 ± 4	51 ± 12 (1.2)	44 ± 6	240 ± 50 (5)	58 ± 7 (1.3)	45.5 ± 11
Epoxidized cyclostreptin	Inactive	Inactive	Inactive	Inactive	Inactive	Inactive
Reduced cyclostreptin	Inactive	Inactive	Inactive	Inactive	Inactive	Inactive

^aIC₅₀ (half-maximal inhibitory concentration) values determined in the ovarian carcinoma lines A2780 (parental line), A2780/AD (an MDR line overexpressing P-glycoprotein), 1A9 (a clone of A2780), and PTX10 and PTX22 (paclitaxel-resistant tubulin mutants derived from 1A9), and in the non-small-cell lung carcinoma line A549. IC₅₀ values were obtained in at least four independent experiments. ^bThe numbers in parentheses are the calculated relative resistance values, obtained by dividing the IC₅₀ value of the resistant line by the IC₅₀ value of the parental line. ND, not determined. Inactive, no inhibition at 5 μM.

the number of micronucleated cells had increased to about 70%. After a 48-h recovery, cyclostreptin-treated cells had somewhat sparser microtubule bundles but an unchanged number of micronucleated cells. After 48 h without drug, paclitaxel-treated cells continued to recover, with micronucleation reduced to about 40%.

We examined the PtK2 cells for DNA content by flow cytometry (Supplementary Table 1 online), and these data also indicated a larger recovery after paclitaxel versus cyclostreptin treatment, with a larger population of G2+M cells persisting after cyclostreptin treatment.

We tested the cytotoxicity of cyclostreptin in paclitaxel-resistant and nonresistant carcinoma cell lines (Table 2). In the nonresistant line, cyclostreptin was around 40 times less active than paclitaxel. However, PTX10 and PTX22, two lines that are resistant to paclitaxel as a result of tubulin mutations, showed lower relative resistance to cyclostreptin (relative resistance index: 27 and 17 for paclitaxel, respectively, and 5 and 1.3 for cyclostreptin, respectively). Moreover, cyclostreptin was highly active in the MDR line, with a resistance factor of 1.2, as compared with resistance factors of 600–900 for paclitaxel and docetaxel.

We performed cell cycle analysis in PtK2, A549, A2780 and A2780/AD cells incubated for 24 h with paclitaxel or cyclostreptin. The lowest concentrations that gave maximal accumulation of cells in the G2+M phase were 0.5 μM, 20 nM, 15 nM and 1 μM, respectively, for paclitaxel, whereas for cyclostreptin this concentration was 100 nM in each of the four cell lines. Thus, cyclostreptin was more active than paclitaxel in the cell lines that are least sensitive to paclitaxel (PtK2 and A2780/AD) (Supplementary Table 1).

Characterization of cyclostreptin binding site by MS

MS chromatograms of digested tubulin samples derived from untreated (Fig. 3a) or cyclostreptin-treated (Fig. 3b) microtubules showed differential, intense peaks corresponding to tubulin peptides producing a cyclostreptin-derived fragment ion at *m/z* 249.0 (see Methods; peaks 1–2 and 3–7 in the trypsin- and chymotrypsin-digested samples, respectively). These signals were absent in control samples (Fig. 3a). MS/MS-based peptide sequencing (Supplementary Fig. 1 online) of peaks 1–7 demonstrated that all peptide sequences map into β-tubulin_{219–243} (Fig. 3c). This sequence contains part of the taxoid site⁷. Peaks 1 and 2 correspond, respectively, to oxidized and nonoxidized cyclostreptin-modified 219-LTTPTYGDLNHLVSATMSG VTTCLR-243. The cyclostreptin-tagged peptide appeared in triply and quadruply charged form in the analyzed mass range. Peaks 3–7 correspond to the sequences indicated (Fig. 3c). A comprehensive study of the fragmentation spectrum from the parent ion corresponding to peak 2 revealed β-tubulin_{219–243} to be the binding site for

cyclostreptin (Supplementary Fig. 1), but the >3 kDa size of this peptide made the precise modification site uncertain. Analysis of the fragmentation spectrum from β-tubulin_{220–230} (peak 5) (Supplementary Fig. 1) and β-tubulin_{220–235} (peak 7) revealed that Thr220 forms a covalent bond with cyclostreptin. Analysis of the fragmentation spectra from the ions corresponding to peaks 3, 4 and 6 (Supplementary Fig. 1) demonstrated a second modification site: Asn228. No doubly labeled peptides were found, so the covalent reactions with Thr220 and Asn228 are mutually exclusive. Although relative areas measured from chromatographic peaks corresponding to chymotryptic peptides from cyclostreptin-treated samples (Fig. 3b) indicate a more extensive reaction with asparagine than with threonine, ionization of chromatographically separated peptides is substantially influenced by the composition of the pool of accompanying peptides eluted at a given retention time. The relative reactivity of the two amino acid residues thus cannot be determined reliably by MS analysis.

However, the chromatographic signal corresponding to 219-LTTPTYGDLNHLVSATMSGVTTCLR-243 showed that there is a 1:1 stoichiometry for the interaction of cyclostreptin with αβ-tubulin in microtubules (Supplementary Fig. 2 online). In the extracted ion chromatography (EIC) for triply charged ions, this peptide was present in one of two alternative forms. Without cyclostreptin, unmodified 219-LTTPTYGDLNHLVSATMSGVTTCLR-243 (*m/z* 884.4 Da) was observed. When cyclostreptin was included in the reaction mixture, only the corresponding peptide with one cyclostreptin added (*m/z* 1,017.6 Da) was observed. Thus, all β-tubulin subunits in the microtubules were modified by addition of a single cyclostreptin.

We performed similar experiments under nonpolymerizing reaction conditions, in which either the heterodimer or small oligomeric species predominate, depending on the Mg²⁺ concentration. Analysis of precursor ion scanning experiments demonstrated the presence of weak chromatographic peaks 1, 2 and 5, but did not detect peaks 3, 4, 6 and 7. Thus, formation of only small amounts of the Thr220 adduct in nonpolymerized tubulin was detectable (from peak intensity, less than 5% with oligomeric tubulin and less than 0.5% with heterodimeric tubulin). To verify these results and increase sensitivity, we also analyzed samples by multiple reaction monitoring (MRM) scan mode, fixing the Q3 quadrupole for the detection of the diagnostic ion at *m/z* 249.0 Da. Ions at *m/z* 1,017.6, 636.8, 816.4 and 779.4 (at the *m/z* of respective chromatographic peaks 2, 4, 5 and 6) were isolated and fragmented. Only precursors and fragmentation spectra from ions corresponding to peaks 2 and 5 were detected (Fig. 3b), which again unambiguously demonstrates the Thr220 modification. We found no

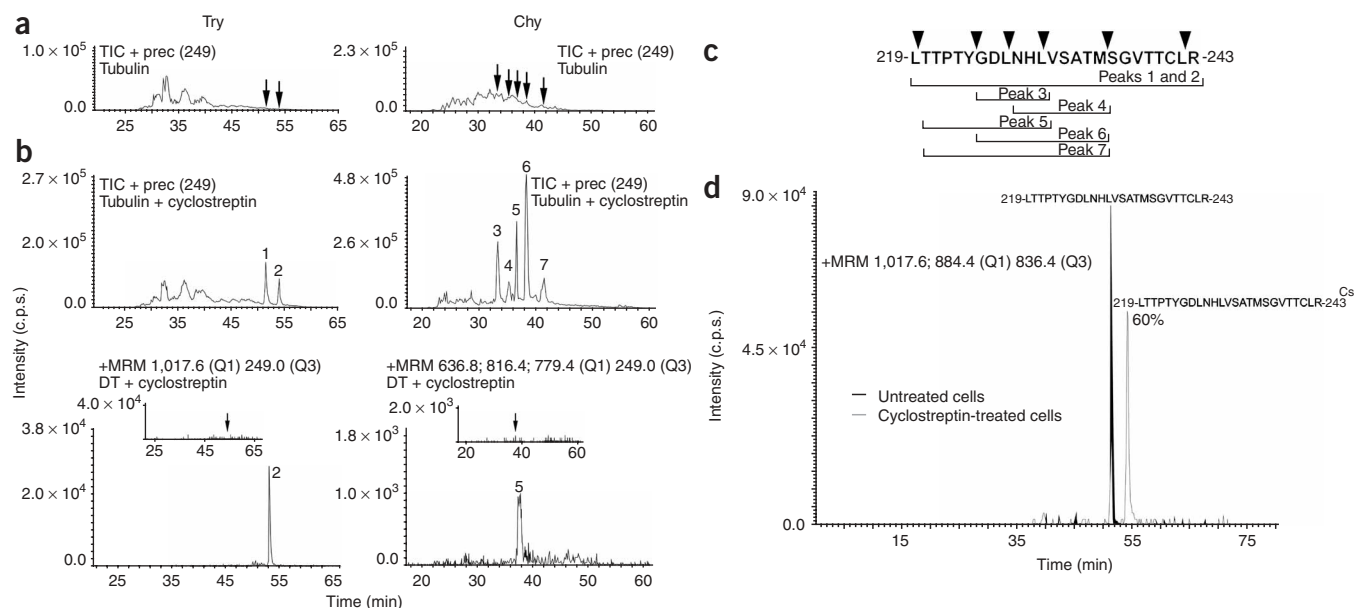


Figure 3 MS analyses of cyclostreptin binding to tubulin. **(a, b)** Total ion chromatogram (TIC) of the precursor ion scanning of fragment at m/z 249.0 from control **(a)** or cyclostreptin-treated **(b)** tubulin samples, digested with trypsin (Try) or chymotrypsin (Chy). The lower panels of **b** show MRM experiments with unassembled, cyclostreptin-treated dimeric tubulin (DT) samples. The upper insets show MRM results for the corresponding dimeric tubulin control samples. Black arrows indicate the retention time expected for signals from peaks 2 (left, trypsin) and 5 (right, chymotrypsin). **(c)** Sequence of β -tubulin₂₁₉₋₂₄₃ containing the amino acids Thr220 and Asn228 labeled with cyclostreptin (we use the sequence nomenclature of ref. 7, which is used extensively in molecular modeling studies). The two cyclostreptin-modified amino acids are actually Thr218 and Asn226 in β -tubulin³¹, and the tryptic peptide actually spans residues 217 to 241). Black triangles indicate the theoretical chymotrypsin cleavage sites within the tryptic peptide. **(d)** MRM experiments with trypsin-digested tubulin extracted from untreated or cyclostreptin-treated cells. Cs, the cyclostreptin tag.

evidence for ions corresponding to peaks 4 and 6, which contain the modified Asn228. The MRM experiments confirmed that the modified peaks are ten-fold more intense in peptides derived from oligomeric versus dimeric tubulin samples.

To verify that the Thr220 modification found in microtubules does not occur in oligomers before microtubule assembly, microtubules stabilized by paclitaxel at a concentration (22 μ M paclitaxel; 20 μ M tubulin) much greater than the 1 μ M drug required to suppress microtubule dynamics¹⁷ were incubated with excess cyclostreptin. This resulted in cyclostreptin displacing paclitaxel from the preformed microtubules. Because paclitaxel binding to microtubules is reversible, cyclostreptin should bind to transiently unoccupied sites, progressively displacing the bound paclitaxel. Therefore, the very same labeling as occurred in the previous experiment when cyclostreptin was added directly to the microtubule assembly mixture is expected, unless the Thr220 modification occurs in oligomers before microtubule assembly, in which case only labeling at Asn228 should be observed. In MRM experiments, ions at m/z 1,017.6, 636.8, 816.4 and 779.4 (peaks 2, 4, 5 and 6, respectively) were detected, whereas in precursor ion scanning experiments, using the ion at m/z 249.0 as the diagnostic signal, we also found tubulin-derived peptides corresponding to peaks 3 and 7. Thus, the modifications at Thr220 and Asn228 were unambiguously documented again. We therefore conclude that the Thr220 modification must occur during the binding of cyclostreptin to microtubules.

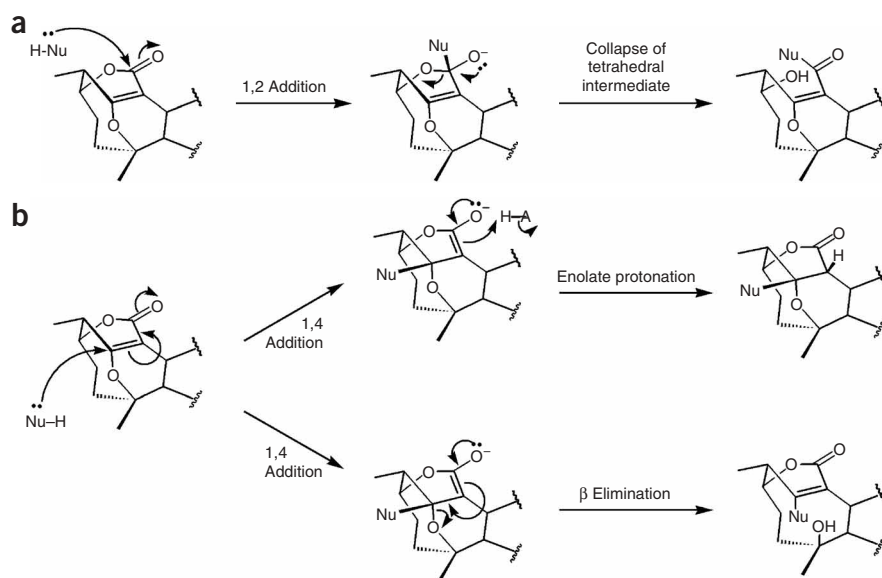
Cyclostreptin labeling of cellular tubulin

To verify that the tubulin-cyclostreptin adduct is formed in treated cells, we incubated A549 cells for 24 h with 1 μ M cyclostreptin or DMSO, isolated their cytoskeletons and digested them with trypsin. We analyzed the digestion mixture by HPLC, with detection by MRM

scan mode for the m/z of the cyclostreptin-labeled form of 219-LTTPTYGDLNHLVSA TMSGVTTCLR-243 (not shown). A peak at the expected retention time for the labeled peptide was detected, which indicates formation of the adduct in living cells.

To determine the proportion of cellular tubulin that had reacted with cyclostreptin, we purified tubulin from cyclostreptin-treated and control A549 cells using a one-step ion-exchange procedure. This method yielded tubulin of >90% purity (Supplementary Fig. 3 online), which is suitable for MS procedures. After treatment with trypsin, the reaction mixture was subjected to HPLC, with analysis in the MRM scan mode with Q1 scanning for the m/z of unmodified and cyclostreptin-linked 219-LTTPTYGDLNHLVSA TMSGVTTCLR-243 (peak 2) and Q3 scanning for a common peptide in the γ -fragmentation series of both labeled and unlabeled peptide (Fig. 3d). Whereas tubulin from control cells showed only one peak, with an m/z of 884.4 (which corresponds to triply charged unmodified peptide), tubulin from cyclostreptin-treated cells showed two peaks. The major peak, with an m/z of 1,017.6, corresponded to the triply charged peptide crosslinked to cyclostreptin, and the minor peak was identical to the unmodified peptide from control cells. The areas of the peaks derived from tubulin in control and cyclostreptin-treated cells indicated that about 60% of the tubulin from treated cells contained the adduct. About 60% of tubulin in paclitaxel-treated 1A9 cells forms polymer¹⁸, a proportion that is not very different from the proportion of tubulin that reacts with cyclostreptin in A549 cells. This suggests near total formation of cyclostreptin adduct in the microtubules of treated A549 cells.

Further, we found that both Thr220 and Asn228 were covalently modified in the tubulin we obtained from cyclostreptin-treated cells. We did this by digesting the isolated tubulin with chymotrypsin. The digest was subjected to HPLC, with analysis in the MRM mode with Q1 scanning for signals at m/z 636.8, 816.4 and 779.4 (corresponding



Scheme 1 Possible reaction mechanisms between cyclostreptin and nucleophiles. (a) Acylation reaction of the lactone through nucleophilic attack at C1. (b) Simple addition of the nucleophile to C17 (top); addition-elimination of the nucleophile at the C2-C17 bond, with formation of a nine-membered ring alcohol (bottom).

respectively to peaks 4, 5 (both containing the Thr220 modification) and 6 (containing the Asn228 modification) and Q3 scanning for the 249.0 signal, which is diagnostic of the covalent reaction with cyclostreptin (Supplementary Fig. 3). The HPLC trace showed the presence of the three peaks, confirming that reactions had occurred with both amino acids.

Cyclostreptin activity requires the strained olefin

The chemical structure of cyclostreptin (Fig. 1a) is characterized by a highly strained olefin (C2-C17). C17 and the lactone carbonyl C1 have been proposed as electrophilic sites that could react covalently with proteins¹⁹.

In principle, cyclostreptin could undergo nucleophilic attack at either of these carbons (Scheme 1), thereby resulting in an increase in the mass of the peptide that is exactly coincident with the mass of cyclostreptin. Both an acylation reaction of the lactone through nucleophilic attack on C1 (Scheme 1a) and a simple addition of nucleophile to C17, with concomitant release of the strain created by the C2-C17 bridgehead alkene, are reasonable modes of covalent bond formation (Scheme 1b). A third possibility is an addition-elimination sequence of the nucleophile at the C2-C17 bond. This would result in the formation of a nine-membered ring alcohol (Scheme 1b). Modification of other reactive groups of cyclostreptin, with the exception of the unstrained C10-C11 olefin bond, would imply the loss of a water molecule.

An extensive study of the reactivity of the strained olefin of cyclostreptin with model nucleophiles²⁰ led to the conclusion that the reaction is a simple addition of the nucleophile to C17 driven by strain release. Generally, the reaction was quantitative, as determined by NMR analysis of reaction mixtures, and no evidence for a nine-membered ring product was found. Both the threonine and the asparagine of the peptide have nucleophilic side chains that might attack cyclostreptin at C17 by an analogous addition reaction.

To confirm that the reaction site is the C2-C17 olefin, we prepared two cyclostreptin analogs. First, the double bond was epoxidized (9,

Fig. 1a), yielding an inactive compound²¹ (Flutax-2 binding unaltered; no activity against cultured cells (Table 2)). Second, the C2-C17 olefin bond was reduced (10, Fig. 1a), again eliminating the biological activities of cyclostreptin (no effect on cell proliferation (Table 2) or Flutax-2 binding; no covalent adduct formed with microtubules as determined by MS). Though the epoxide is potentially electrophilic at C1, C2 and C17, reduced cyclostreptin no longer has the strained olefin; only C1 is a potential electrophile. However, the inactivity of these two analogs buttresses the conclusion that it is the strained olefin of cyclostreptin that reacts with tubulin through a simple addition at C17, as previously demonstrated with model nucleophiles²⁰.

Molecular modeling

The complex of cyclostreptin with Thr220 was modeled *in silico* by forming a covalent bond with its side chain oxygen (Supplementary Fig. 4 online). We optimized the resulting adduct with MacroModel (Schrödinger), thereby identifying a possible binding site formed by residues 217–223 and 277–279 from β -tubulin, 323–328 from the adjacent α -tubulin, 95–99 from β -tubulin of a neighboring protofilament, and 128–132 from α -tubulin of a neighboring protofilament (Supplementary Fig. 4). Assuming this complex represents that observed experimentally, there are two additional hydrogen bonding interactions that would help stabilize the complex: the hydroxyl group at C15 with Arg278 and the C1 carbonyl group with Thr221. This adduct is further stabilized by hydrophobic contacts with a nonpolar region of the adjacent α -tubulin (Gln128-Leu132).

Cyclostreptin also reacts with Asn228. The atoms of the backbone of this amino acid are located at the luminal taxoid site, and the side chain forms two strong hydrogen bonds with the exchangeable nucleotide. Therefore, either the position of the Asn228 side chain in microtubules differs from its position in zinc-induced sheets^{7,8}, or cyclostreptin causes the displacement of the Asn228 side chain by forming a noncovalent precomplex at the paclitaxel site, thereby facilitating a subsequent reaction of cyclostreptin with the Asn228 side chain amide.

DISCUSSION

Cyclostreptin contains two electrophilic functional groups: a strained bridgehead olefin and a lactone carbonyl group. Other natural products containing such moieties react covalently with nucleophilic residues in protein active sites, thereby causing biological effects^{22,23}.

The biological activities of cyclostreptin overwhelmingly favor microtubules as the target of the compound. However, it is not a classical taxoid-site ligand. Despite strongly displacing taxoid-site ligands from microtubules, it only weakly induces microtubule assembly^{5,6,13}.

Our results show that cyclostreptin binds covalently to microtubules. Cyclostreptin is the first MSA that has been shown to do so and the first taxoid-site ligand whose binding to dimeric tubulin has been detected. MS analysis showed that in microtubules cyclostreptin forms a covalent bond with either Thr220 or Asn228. We found that in unpolymerized tubulin, only Thr220 forms a bond with

cyclostreptin, and this covalent interaction is much less extensive than the reaction with microtubules. We also demonstrated that both crosslinks to β -tubulin form in cyclostreptin-treated cells. Covalent bond formation explains the unusual biochemical properties of cyclostreptin, such as the distinct requirement for higher temperatures for assembly induction and binding to polymer and the high stability of cyclostreptin polymer to disassembly at 0 °C⁶. Once covalently bound to microtubules, cyclostreptin cannot dissociate and the microtubules cannot disassemble, as they are more stable than untreated control and paclitaxel-induced microtubules.

Similarly, we found that PtK2 cellular microtubule bundles induced by cyclostreptin are more stable than those induced by paclitaxel. Although cyclostreptin is 40-fold less cytotoxic than paclitaxel, it retains its activity in cells that are resistant to paclitaxel by over-expression of P-glycoprotein or by expression of mutant β -tubulins, becoming more potent than paclitaxel in the former case. Therefore, formation of a covalent tubulin adduct can be a mechanism to escape these mechanisms of resistance, at least in cultured cells. Though agents that react covalently with specific targets can be too toxic for use in humans²⁴, some covalently reactive compounds are successfully used in the clinic. Examples are the antiobesity drug tetrahydrolipstatin, which reacts with pancreatic lipase²⁵, and the anticancer platinum agents, which react with DNA²⁶. In the MDR A2780/AD cells, we found that the covalent adduct of cyclostreptin with tubulin can escape the pump. With the tubulin mutants, cyclostreptin affinity for the altered tubulins might be modified. Alternatively, the longer time frame involved in cell culture studies might still lead to irreversible tubulin inactivation by covalent bond formation, even if the tubulins have reduced affinity for cyclostreptin. In summary, because the formation of the adduct is a kinetically controlled, irreversible process, resistant tumor cells cannot escape the effect of cyclostreptin by reducing its affinity for the target or by enhancing drug efflux, which suggests that the design of ligands that covalently react with the taxoid site or other targets might be an effective way to address drug resistance.

The discovery of the covalent reactions of cyclostreptin with tubulin and microtubules provides new insights into two obscure aspects of the mechanism of ligand binding to the taxoid site. First, modeling of paclitaxel-stabilized zinc sheet protofilaments into a microtubule structure led to the conclusion that the taxoid site is on β -tubulin adjacent to the microtubule lumen^{7,8}. In contrast, kinetic measurements, effects of MAPs and antibody binding^{10,11,15} indicated an easily accessible site, most logically on the outer microtubule surface. To reconcile these observations, we proposed an exterior taxoid binding site to which ligands bind initially, before transfer to the luminal site¹⁰. The two sites could not be occupied simultaneously because of the observed 1:1 binding stoichiometry (similar stoichiometry has been found for discodermolide (M.C.E., unpublished data) and for epothilone A and epothilone B binding¹⁴). The proposed site was at pore type I, including β -tubulin residues Phe214, Thr220, Thr221 and Pro222 in the H6-H7 loop¹⁰. We have now shown that the taxoid-site agent cyclostreptin reacts covalently with Thr220 at the proposed pore type I site, and it also reacts with Asn228, a residue at the luminal site.

The proposed two-step mechanism is consistent with the two-step kinetics of binding of fluorescent taxoids to microtubules¹⁵. Step one is a bimolecular reaction with a micromolar K_d and a k_f of about $10^6 \text{ M}^{-1} \text{ s}^{-1}$, which is most consistent with a diffusion-limited reaction involving an exposed site on the microtubule surface, such as the pore type I site containing Thr220. Step two is a monomolecular reaction with a $K_{eq} \sim 20$, which indicates that about 5% of the bound ligand remains at the external site. The data obtained with the fluorescent

taxoids indicate that the first step involves binding of the taxoid moiety without immobilization of the fluorescein group, as there is no increase in fluorescence anisotropy. This is consistent with the taxoid moiety binding at Thr220, because when the taxoid and fluorescent moieties are separated by a longer linker, the fluorescein moiety is fully accessible to antibodies¹¹.

The hypothesis that binding at the pore type I site, as manifested by the reaction of cyclostreptin with Thr220, precedes binding of taxoid-site agents to the luminal site is supported by the fact that covalent binding of cyclostreptin to microtubules abolishes subsequent binding of every taxoid-site agent examined (Table 1; Fig. 1c). In the Flutax-2 experiment, we incubated 50 nM taxoid with up to 1 μM taxoid sites preincubated with cyclostreptin, and Flutax-2 binding was completely abolished. Even if only 1% of the taxoid sites had been accessible to Flutax-2, a change in the fluorescence anisotropy signal would have been detectable. Cyclostreptin reacts with tubulin in microtubules in a 1:1 proportion, and therefore such microtubules, as the MS data show, would contain $\alpha\beta$ dimers with the β -tubulin modified at both Thr220 and Asn228. Though dimers modified at Asn228 would not have bound Flutax-2 because the taxoid site would have been at least partially occupied by the cyclostreptin moiety, one can imagine other routes to the luminal taxoid site that would be available as a result of modification at Thr220. For example, Flutax-2 might reach the lumen through type II pores or through microtubule ends. The failure to detect even low levels of Flutax-2 binding indicates that an initial interaction at the pore type I site is an obligatory route to the luminal site.

Second, previous studies^{12,27} have shown that paclitaxel binds avidly to microtubules but not to $\alpha\beta$ heterodimers. However, paclitaxel and other taxoid-site agents initiate assembly in tubulin solutions in which no microtubules (that is, presumptive binding sites) exist. It has been proposed that paclitaxel might bind to tubulin oligomers²⁸, thereby leading to assembly under otherwise unfavorable conditions. In the present work, we found a low level of cyclostreptin covalent reactivity with Thr220 in dimeric and oligomeric tubulin, under conditions in which microtubule assembly is prevented by keeping the free Mg^{2+} concentration lower than that required to assemble microtubules with 20 μM tubulin¹². This demonstrates an MSA binding site in non-assembled tubulin. No reaction with Asn228 was observed, which indicates that the luminal site is not present without microtubule formation. The binding affinity of MSAs for the site containing Thr220 in $\alpha\beta$ heterodimers and oligomers must be very low, but binding to this site might initiate an assembly reaction, with creation of the higher affinity luminal site and stabilization of nascent polymer. The irreversible covalent reaction of cyclostreptin with Thr220 allows trapping of the binding complex and detection of this evanescent species.

The assembly process might involve transformation of some elements from acting as components of the external site into acting as part of the luminal site. However, the Thr220 cyclostreptin adduct forms under all reaction conditions examined, including in pre-formed, paclitaxel-stabilized microtubules following paclitaxel displacement by cyclostreptin. Thus, the external pore type I site must also exist to some extent after assembly. Overall, the data presented here demonstrate the existence of an MSA binding site in unassembled tubulin and support the hypothesis that taxoids reach the luminal site through transient binding to the pore type I site.

METHODS

Previously described methodologies. Previous papers provide details for preparation of tubulin²⁹, cyclostreptin²⁰, epoxidized cyclostreptin²¹ and glutaraldehyde-stabilized microtubules, and also for quantitation of the taxoid sites of glutaraldehyde-stabilized microtubules^{10,14}, electron microscopy, radioactively

labeled ligand binding studies⁶, cytotoxicity assays and cell cycle analysis⁵, and culture and immunofluorescence analysis of PtK2 potaroo kidney cells³⁰. We cultured human ovarian carcinoma 1A9, PTX10 and PTX22¹⁸ and lung carcinoma A549 cells as previously described⁵, and we grew A2780 and A2780/AD (P-glycoprotein overexpressing) cells in the same medium supplemented with 0.25 units ml⁻¹ of bovine insulin.

Ligands. See **Supplementary Methods** online for preparation of reduced cyclostreptin and information about other ligands.

Binding of cyclostreptin to microtubules. We incubated samples containing crosslinked microtubules (35 μ M taxoid sites) and 30 μ M cyclostreptin for 30 min at 25 °C in GAB (3.4 M glycerol, 10 mM NaP_i, 1 mM EGTA and 6 mM MgCl₂, pH 6.7) plus 0.1 mM GTP. Samples were processed and extracted, with each organic extract residue dissolved in 200 μ l of CH₃OH¹⁴. For uncrosslinked microtubules, samples were prepared using 20 μ M tubulin plus 25 μ M cyclostreptin in GAB plus 1 mM GTP.

Ligands reversibly bound to pelleted polymer and ligands in the supernatant were detected by HPLC-MS (**Supplementary Methods**).

Inhibition of binding of Flutax-2 to microtubules. We incubated crosslinked microtubules (60 μ M) with 66 μ M cyclostreptin, epoxidized cyclostreptin, reduced cyclostreptin or 1.3% DMSO overnight at 22 °C in GAB plus 0.1 mM GTP and dialyzed for 5 h against the same solution. Flutax-2 (50 nM) was titrated with these preparations, and K_{a s for Flutax-2 binding were calculated¹⁴.

We also performed competition of cyclostreptin with Flutax-2 with native PtK2 cytoskeletons stained for 10 min with 0.2 μ M Flutax-2, washed (8 \times) in two wells with 2 ml of 10 mM PIPES, 1 mM EGTA, 1 mM MgCl₂, 4% PEG, pH 6.8 and incubated for 15 min with 100 μ M cyclostreptin, paclitaxel or 2% DMSO. After washing again, coverslips were mounted and examined. Cytoskeletons were also preincubated with 10 μ M cyclostreptin, paclitaxel or 1% DMSO for 10 min, washed, stained with 0.2 μ M Flutax-2 and visualized.

Flutax-2 dissociation kinetics. The dissociation kinetics of Flutax-2 from microtubules was measured by fluorescence anisotropy (**Supplementary Methods**).

Purification of tubulin from cells. We incubated five 175-cm² flasks with a monolayer of A549 cells for 24 h with 1 μ M cyclostreptin or 0.1% DMSO. Cells were removed with phosphate-buffered saline (PBS) and 0.5 mM EDTA, washed with PBS and harvested by centrifugation. The cell pellet (1 ml) was resuspended in 1 ml of 10 mM NaP_i, 1 mM MgCl₂, 0.1 mM GTP, 0.24 M sucrose, pH 7.0 and stored in liquid nitrogen. After thawing the cells, DTT and GTP were added to 1 mM, and the cells were hand-homogenized in glass. The homogenate was centrifuged (38,000 r.p.m., 1 h, 4 °C, TLA 100.4 rotor in an Optima TLX ultracentrifuge). The supernatant was adjusted to 0.4 M KCl and loaded onto a HiTrap DEAE Fast Flow 1 ml column in an FPLC system (GE Healthcare) developed at 1 ml min⁻¹. Unbound protein was removed with 5 ml of 10 mM NaP_i, 1 mM MgCl₂, 0.1 mM GTP, 0.4 M KCl, pH 7.0. Bound protein was eluted with 0.8 M KCl in the same buffer and desalted into 10 mM NaP_i, 1 mM MgCl₂, 0.1 mM GTP, pH 7.0 with a HiTrap desalting column (GE Healthcare). The tubulin was 90% pure, as determined by SDS-PAGE. The tubulin was stored in liquid nitrogen after addition of 0.24 M sucrose.

Protein digestion and sample preparation for MS analysis. We prepared tubulin control, cyclostreptin-treated, and reduced cyclostreptin-treated samples using native microtubules polymerized for 30 min at 37 °C in GAB plus 1 mM GTP (200 μ l, 20 μ M tubulin with 2.5% DMSO or 25 μ M drug). In another sample, 20 μ M tubulin in GAB plus 1 mM GTP was assembled with 22 μ M paclitaxel for 15 min at 37 °C (>97% assembly⁵) and incubated for another 45 min at 37 °C after addition of 50 μ M cyclostreptin to displace bound paclitaxel. Morphology of polymers was always verified to be microtubules. Microtubules were harvested by centrifugation as described above. Pellets were washed twice with water and suspended in 200 μ l of 50 mM NH₄HCO₃, 12 mM EDTA, 0.01% SDS, pH 7.6. Unassembled tubulin samples were prepared using 20 μ M GTP-tubulin in 10 mM NaP_i, 1 mM EDTA, 0.1 mM GTP, pH 7.0 without (for dimeric tubulin) or with (for oligomeric tubulin) 1.5 mM MgCl₂ and 2.5% DMSO or 25 μ M cyclostreptin. Samples

were centrifuged as described above to remove aggregates, and 20 μ l was diluted 1:1 into 50 mM NH₄HCO₃ and digested with trypsin (1 μ g sequencing grade, Promega, 2 h, 37 °C) or chymotrypsin (1 μ g type VII, TLCK treated, Sigma, 1 h, 25 °C). Reaction mixtures were dried *in vacuo* and, for analysis, dissolved in 5% CH₃CN, 0.5% CH₃COOH.

Nano-HPLC and tandem triple quadrupole MS analysis of peptides.

We analyzed peptide solutions from control, cyclostreptin-treated and reduced cyclostreptin-treated samples with a Supelco C18 nanocolumn developed with a CH₃CN gradient. Peptides were eluted into a Protana nanospray ion source and the resulting ions were analyzed on the 4000 Q Trap system (Applied Biosystems) as described in **Supplementary Methods**.

MRM. MRM of selected cyclostreptin-bound peptides derived from unassembled tubulin and tubulin isolated from cells is described in **Supplementary Methods**.

Detection of cyclostreptin labeling of tubulin by nano-HPLC coupled to three-dimensional ion-trap MS. We injected tryptic peptides from control and cyclostreptin-treated microtubules onto a Supelco C18 nanocolumn. A CH₃CN gradient was used to elute peptides to a PicoTip emitter nanospray needle (New Objective) for real-time ionization and peptide fragmentation on an Esquire HCT ion-trap (Bruker Daltonics) mass spectrometer (**Supplementary Methods** and **Supplementary Fig. 5** online).

MS data analysis. We analyzed all chromatograms and MS/MS spectra from the 4000 Q Trap system with Analyst 1.4.1 (Applied Biosystems). All HPLC-MS/MS experiments were repeated with five independent samples. Chromatographic and MS data from the three-dimensional ion-trap system were processed by DataAnalysis 3.3 (Bruker Daltonics).

Molecular modeling of cyclostreptin binding to tubulin. We performed the simulations needed to investigate the covalent binding of cyclostreptin with MacroModel 8.5 (Schrödinger) over a model of pore type I that was built from the structure 1JFF in the Protein Data Bank.

Accession codes. Protein Data Bank: the structure 1JFF was used to model pore type I in MacroModel 8.5.

Requests for materials. cdv@uci.edu.

Note: Supplementary information and chemical compound information are available on the Nature Chemical Biology website.

ACKNOWLEDGMENTS

The authors thank J. Villarrasa for helpful discussions, P. Lastres for his help with flow cytometry, and Matadero Madrid Norte S.A. and José Luis Gancedo S.L. for providing calf brains for tubulin purification. This work was supported in part by grant BFU2004-00358 from Ministerio de Educación y Ciencia and grant 200520M061 from Comunidad Autónoma de Madrid to J.E.D. R.M.B. was supported by a Beca de Formación de Profesorado Universitario del Ministerio de Educación y Ciencia fellowship.

AUTHOR CONTRIBUTIONS

R.M.B. performed research; E.C. performed research; I.B. designed and performed research; O.P. performed research; M.C.E. performed research; R.M. performed research; G.C. performed research; C.D.V. contributed materials and performed research; B.W.D. contributed materials and edited the manuscript; E.J.S. contributed materials; J.A.L. interpreted data; J.M.A. designed research, interpreted data and edited the manuscript; E.H. interpreted data and wrote the paper; J.E.D. designed and performed research, interpreted data and wrote the paper.

COMPETING INTERESTS STATEMENT

The authors declare that they have no competing financial interests.

Published online at <http://www.nature.com/naturechemicalbiology>
Reprints and permissions information is available online at <http://npg.nature.com/reprintsandpermissions>

- Jordan, M.A. & Wilson, L. Microtubules as a target for anticancer drugs. *Nat. Rev. Cancer* **4**, 253–265 (2004).

2. Jordan, M.A., Toso, R.J., Thrower, D. & Wilson, L. Mechanism of mitotic block and inhibition of cell proliferation by taxol at low concentrations. *Proc. Natl. Acad. Sci. USA* **90**, 9552–9556 (1993).
3. Schiff, P.B., Fant, J. & Horwitz, S.B. Promotion of microtubule assembly *in vitro* by taxol. *Nature* **277**, 665–667 (1979).
4. Díaz, J.F. & Andreu, J.M. Assembly of purified GDP-tubulin into microtubules induced by taxol and taxotere: reversibility, ligand stoichiometry, and competition. *Biochemistry* **32**, 2747–2755 (1993).
5. Buey, R.M. *et al.* Microtubule interactions with chemically diverse stabilizing agents: thermodynamics of binding to the paclitaxel site predicts cytotoxicity. *Chem. Biol.* **12**, 1269–1279 (2005).
6. Edler, M.C. *et al.* Cyclostreptin (FR182877), an antitumor tubulin-polymerizing agent deficient in enhancing tubulin assembly despite its high affinity for the taxoid site. *Biochemistry* **44**, 11525–11538 (2005).
7. Nogales, E., Wolf, S.G. & Downing, K.H. Structure of the $\alpha\beta$ -tubulin dimer by electron crystallography. *Nature* **391**, 199–203 (1998).
8. Nogales, E., Whittaker, M., Milligan, R.A. & Downing, K.H. High-resolution model of the microtubule. *Cell* **96**, 79–88 (1999).
9. Giannakakou, P. *et al.* A common pharmacophore for epothilone and taxanes: molecular basis for drug resistance conferred by tubulin mutations in human cancer cells. *Proc. Natl. Acad. Sci. USA* **97**, 2904–2909 (2000).
10. Díaz, J.F., Barasoain, I. & Andreu, J.M. Fast kinetics of taxol binding to microtubules. Effects of solution variables and microtubule-associated proteins. *J. Biol. Chem.* **278**, 8407–8419 (2003).
11. Díaz, J.F., Barasoain, I., Souto, A.A., Amat-Guerri, F. & Andreu, J.M. Macromolecular accessibility of fluorescent taxoids bound at a paclitaxel binding site in the microtubule surface. *J. Biol. Chem.* **280**, 3928–3937 (2005).
12. Díaz, J.F., Menendez, M. & Andreu, J.M. Thermodynamics of ligand-induced assembly of tubulin. *Biochemistry* **32**, 10067–10077 (1993).
13. Sato, B. *et al.* A new antimitotic substance, FR182877. I. Taxonomy, fermentation, isolation, physico-chemical properties and biological activities. *J. Antibiot. (Tokyo)* **53**, 123–130 (2000).
14. Buey, R.M. *et al.* Interaction of epothilone analogs with the paclitaxel binding site; relationship between binding affinity, microtubule stabilization, and cytotoxicity. *Chem. Biol.* **11**, 225–236 (2004).
15. Díaz, J.F., Strobe, R., Engelborghs, Y., Souto, A.A. & Andreu, J.M. Molecular recognition of taxol by microtubules. Kinetics and thermodynamics of binding of fluorescent taxol derivatives to an exposed site. *J. Biol. Chem.* **275**, 26265–26276 (2000).
16. Barshop, B.A., Wrenn, R.F. & Frieden, C. Analysis of numerical methods for computer simulation of kinetic processes: development of KINSIM—a flexible, portable system. *Anal. Biochem.* **130**, 134–145 (1983).
17. Derry, W.B., Wilson, L. & Jordan, M.A. Substoichiometric binding of taxol suppresses microtubule dynamics. *Biochemistry* **34**, 2203–2211 (1995).
18. Giannakakou, P. *et al.* Paclitaxel-resistant human ovarian cancer cells have mutant β -tubulins that exhibit impaired paclitaxel-driven polymerization. *J. Biol. Chem.* **272**, 17118–17125 (1997).
19. Adam, G.C., Vanderwal, C.D., Sorensen, E.J. & Cravatt, B.F. (–)-FR182877 is a potent and selective inhibitor of carboxylesterase-1. *Angew. Chem. Int. Edn Engl.* **42**, 5480–5484 (2003).
20. Vanderwal, C.D., Vosburg, D.A., Weiler, S. & Sorensen, E.J. An enantioselective synthesis of FR182877 provides a chemical rationalization of its structure and affords multigram quantities of its direct precursor. *J. Am. Chem. Soc.* **125**, 5393–5407 (2003).
21. Yoshimura, S., Sato, B., Kinoshita, T., Takase, S. & Terano, H. A new antimitotic substance, FR182877. III. Structure determination. *J. Antibiot. (Tokyo)* **53**, 615–622 (2000).
22. Hadvary, P., Sidler, W., Meister, W., Vetter, W. & Wolfer, H. The lipase inhibitor tetrahydropipstatin binds covalently to the putative active site serine of pancreatic lipase. *J. Biol. Chem.* **266**, 2021–2027 (1991).
23. Liu, S., Widom, J., Kemp, C.W., Crews, C.M. & Clardy, J. Structure of human methionine aminopeptidase-2 complexed with fumagillin. *Science* **282**, 1324–1327 (1998).
24. Evans, D.C., Watt, A.P., Nicoll-Griffith, D.A. & Baillie, T.A. Drug-protein adducts: an industry perspective on minimizing the potential for drug bioactivation in drug discovery and development. *Chem. Res. Toxicol.* **17**, 3–16 (2004).
25. Hennessy, S. & Perry, C.M. Orlistat: a review of its use in the management of obesity. *Drugs* **66**, 1625–1656 (2006).
26. Brabec, V. & Kasparkova, J. Modifications of DNA by platinum complexes. Relation to resistance of tumors to platinum antitumor drugs. *Drug Resist. Updat.* **8**, 131–146 (2005).
27. Parness, J. & Horwitz, S.B. Taxol binds to polymerized tubulin *in vitro*. *J. Cell Biol.* **91**, 479–487 (1981).
28. Díaz, J.F., Andreu, J.M., Diakun, G., Towns-Andrews, E. & Bordas, J. Structural intermediates in the assembly of taxoid-induced microtubules and GDP-tubulin double rings: time-resolved X-ray scattering. *Biophys. J.* **70**, 2408–2420 (1996).
29. Weisenberg, R.C., Borisy, G.G. & Taylor, E.W. The colchicine-binding protein of mammalian brain and its relation to microtubules. *Biochemistry* **7**, 4466–4479 (1968).
30. Andreu, J.M. & Barasoain, I. The interaction of baccatin III with the taxol binding site of microtubules determined by a homogeneous assay with fluorescent taxoid. *Biochemistry* **40**, 11975–11984 (2001).
31. Krauhs, E. *et al.* Complete amino acid sequence of β -tubulin from porcine brain. *Proc. Natl. Acad. Sci. USA* **78**, 4156–4160 (1981).